



Unraveling Structural Phase Transformation by Simultaneously Determining the Lattice Constants and Mismatch Angle in VO₂/Al₂O₃ Epitaxial Thin Films

OPEN ACCESS

Edited by:

Xiaoning Li,
University of Wollongong, Australia

Reviewed by:

Hangwen Guo,
Fudan University, China
Taisong Pan,
University of Electronic Science and
Technology of China, China

*Correspondence:

Hui Zhang
huiz@ustc.edu.cn
Yuanjun Yang
yangyuanjun@hfut.edu.cn

[†]These authors have contributed
equally to this work

Specialty section:

This article was submitted to
Quantum Materials,
a section of the journal
Frontiers in Materials

Received: 31 January 2022

Accepted: 07 March 2022

Published: 22 March 2022

Citation:

Liu Y, Wang C, Huang W, Wang S,
Qiu H, Ge W, Chen M, Zhang H, Gu Y,
Zhang X, Li X, Gao X and Yang Y (2022)
Unraveling Structural Phase
Transformation by Simultaneously
Determining the Lattice Constants and
Mismatch Angle in VO₂/Al₂O₃ Epitaxial
Thin Films.
Front. Mater. 9:866468.
doi: 10.3389/fmats.2022.866468

Yichao Liu^{1†}, Cangmin Wang^{1†}, Wenyu Huang¹, Shaoting Wang², Huaili Qiu¹, Weifeng Ge¹, Meixia Chen¹, Hui Zhang^{3*}, Yueliang Gu⁴, Xingmin Zhang⁴, Xiaolong Li⁴, Xingyu Gao⁴ and Yuanjun Yang^{1*}

¹Department of Physics, School of Physics, Hefei University of Technology, Hefei, China, ²School of Microelectronics, Hefei University of Technology, Hefei, China, ³Department of Physics, University of Science and Technology of China, Hefei, China, ⁴Shanghai Synchrotron Radiation Facility (SSRF), Shanghai Advanced Research Institute, Chinese Academy of Sciences, Shanghai, China

As a prototype of a strongly correlated electron system, bulk vanadium dioxide (VO₂) exhibits a large and reversible metal–insulator transition (MIT) near 340 K, concomitantly accompanied by a monoclinic–rutile structural phase transformation (SPT). In this study, we systematically investigated the SPT across the MIT in a (010)-VO₂/(0001)-Al₂O₃ epitaxial thin film by simultaneously determining three lattice constants (*a*, *b*, and *c*) and the mismatch angle ($\Delta\beta$) using high-resolution X-ray diffraction. The lattice constants *a*, *b*, and *c* were approximately 5.723, 4.521, and 5.393 Å, respectively, at room temperature, and the mismatch angle was approximately 122.02°. As the temperature increased, the lattice constants and mismatch angle did not change significantly until the temperature reached the MIT point. Then, *a*, *b*, and *c* suddenly increased to approximately 5.689 Å, 4.538 Å, and 5.411 Å, respectively, and retained this value up to nearly 90°C. However, the mismatch angle first slightly increased and then sharply decreased to 122.00°. Additionally, the lattice constants and mismatch angle were almost reproducible with decreasing temperature, except for hysteresis in the MIT region. These results verify that VO₂ undergoes an MIT, simultaneously accompanied by SPT, in thicker films with small strain and weak substrate constraints, analogous to bulk VO₂. This was further confirmed by *in-situ* varying-temperature Raman characterization. These findings provide insights into the SPT and reveal an angular parameter for judging the SPT in VO₂ systems.

Keywords: metal-insulator transition, structural phase transformation, VO₂ epitaxial film, lattice constants and mismatch angle, high-resolution X-ray diffraction

INTRODUCTION

Since Morin first discovered the metal–insulator transition (MIT) behavior in 1959, vanadium oxide (VO₂) has attracted great attention owing to its implications in the fundamental sciences and potential technological applications (Morin, 1959; Mott, 1990; Stefanovich et al., 2000; Lysenko et al., 2006; Park et al., 2007; Nakajima et al., 2008; Kevin Wang et al., 2013; Lee et al., 2017; Shi and Chen, 2018; Wall et al., 2018). Bulk VO₂ undergoes a thermally-induced MIT with a critical temperature near 340 K, accompanied by a structural phase transformation (SPT) from a low-temperature insulating phase to a high-temperature metallic phase (Mott, 1990; Lee et al., 2017; Shi and Chen, 2018; Wall et al., 2018). Simultaneously, large and reversible changes in electrical (Stefanovich et al., 2000), optical (Lysenko et al., 2006; Nakajima et al., 2008), magnetic (Park et al., 2007), and thermal (Kevin Wang et al., 2013) properties can be achieved in the vicinity of the MIT. In addition, the MIT behavior of VO₂ is easily modulated by external stimuli, such as temperature (Liu et al., 2015), strain (Cao et al., 2009; Hu et al., 2010; Aetukuri et al., 2013; Lee et al., 2015), light (Morrison et al., 2014), and electric fields (Nakano et al., 2012; Jeong et al., 2013; Sharma et al., 2018), enabling broad applications in energy saving (Imada et al., 1998), photoelectric switching (Huang et al., 2010), smart windows (Ning Wang et al., 2013; Zhou et al., 2013), infrared devices (Chen et al., 2004), and information storage media (Driscoll et al., 2009; Pellegrino et al., 2012). However, the mechanism of the MIT in VO₂ remains unclear; to date, there are three main perspectives. First, strong electron–electron correlation dominantly drives the Mott transition in the VO₂ system (Jeong et al., 2013). Second, the electron–phonon mechanism is structurally driven by the Peierls transition (Baum et al., 2007). The third involves the combined action of electron correlation and structural instability (Yao et al., 2010; Cocker et al., 2012). Regardless of the specific mechanism behind different VO₂ systems [for example, strained, relaxed in the film state (Lee et al., 2018), or nanostructured samples (Cao et al., 2009)], the SPT is the key link to uncovering the MIT mechanism in VO₂.

Extensive studies have been conducted on the SPT and crystal structure of VO₂ films, with recent advances in their preparation and growth (Fan et al., 2012; Yu et al., 2017; Lee et al., 2018; Sharma et al., 2018; Zhang et al., 2020). Fan et al. analyzed the structural domain-matching epitaxy relationship between VO₂ and a sapphire substrate (Fan et al., 2012), which may be important for understanding the MIT mechanism. Yu et al. obtained VO₂ thin films using an oxygen annealing treatment and achieved an insulating monoclinic phase. Moreover, the oxidation conditions affect the microstructure of VO₂ films and further modulate its MIT performance (Yu et al., 2017). Lee et al. demonstrated an isostructural, purely electronically driven MIT in VO_{2.8}/VO₂ bilayers on (001)-TiO₂ substrates (Lee et al., 2018). Sharma et al. observed the crucial role of oxygen vacancies in controlling the MIT in epitaxial VO₂ thin films on Nb-doped TiO₂ substrates (Sharma et al., 2018). Zhang et al. compared the crystal structure and optical properties of VO₂ thin films on silicon, quartz, and sapphire substrates, revealing their distinct behaviors (Zhang et al., 2020). Despite the

mentioned research, SPT across the MIT in VO₂ thin films is insufficiently understood. To date, in thin-film VO₂ systems, the structural unit cell parameters a , b , c and β have not been simultaneously determined to directly reveal SPT behaviors across the MIT.

In this study, we deposited a VO₂ thin film on a c -plane sapphire substrate using radio-frequency (RF) magnetron sputtering. The epitaxial relationship between VO₂ and the Al₂O₃ substrate, and temperature-dependent crystal structure evolution were revealed using high-resolution X-ray diffraction (XRD). The lattice constants and mismatch angle of the VO₂ film were simultaneously determined to reveal the SPT across the MIT, indicating a distinct phase transition compared to the bulk VO₂ system (single crystal or polycrystal).

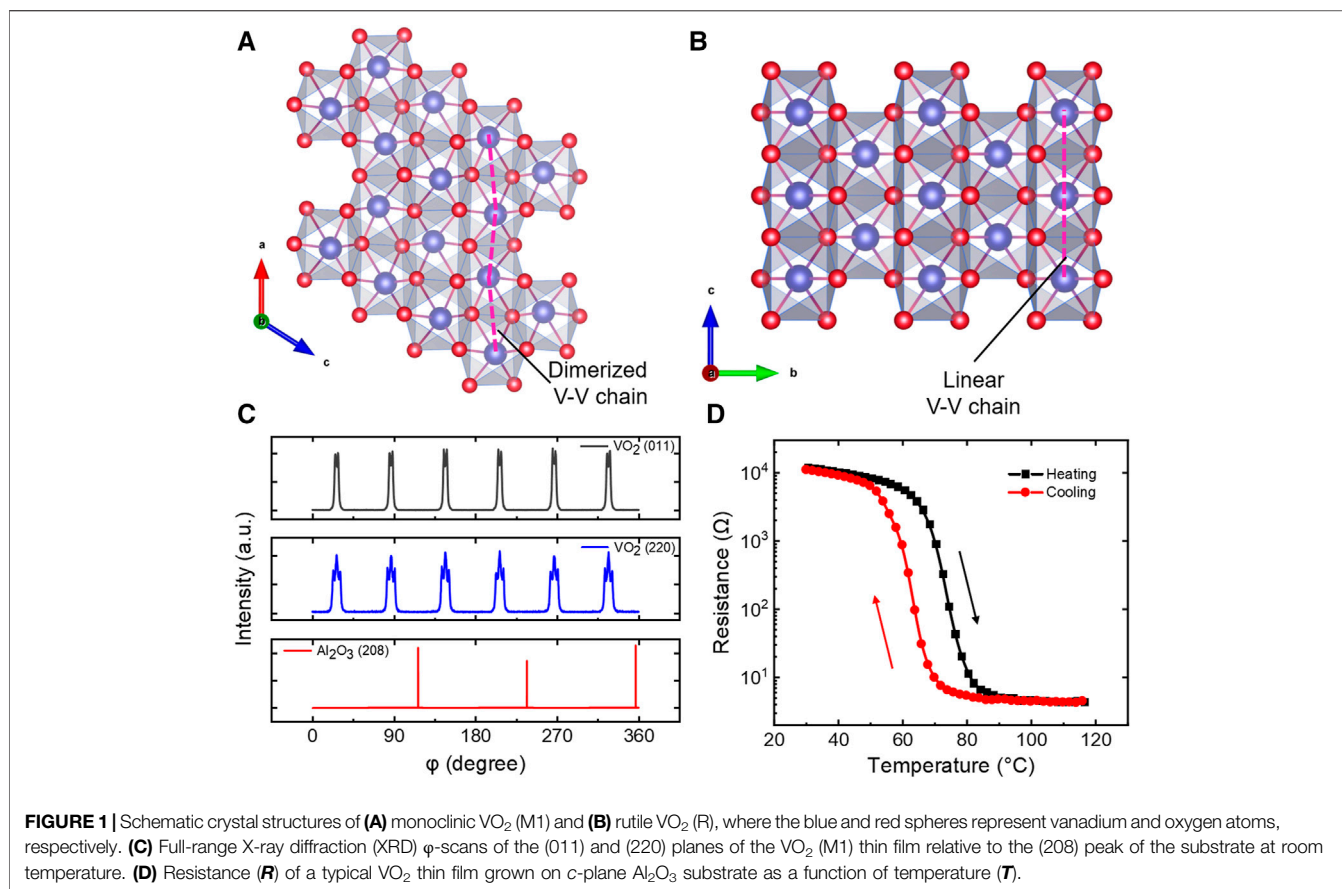
EXPERIMENTAL METHODS

We deposited VO₂ thin films on (0001)-Al₂O₃ single-crystal substrates with dimensions of 5 × 5 × 0.5 mm using a reactive RF magnetron sputtering technique. A circular vanadium metal target with a purity of 99.99% was sputtered. The RF power was set to 65 W, and the gas pressure was approximately 0.33 Pa. The argon (Ar) and oxygen (O₂) flow ratio was set to 50:1.5, and the substrate temperature was set to 520°C. The sputtering distance was approximately 12 cm, and the background pressure was pumped to a value greater than 2.5 × 10⁻⁴ Pa. The film thickness was determined to be approximately 90 nm by controlling the deposition time (Yang et al., 2015a). The orientation, structure, and epitaxial quality of the VO₂ thin films were characterized using high-resolution XRD in house with Cu K α_1 and partially on the 14B beamline of the Shanghai Synchrotron Radiation Facility (SSRF) with an X-ray wavelength of ~1.2395 Å. The HORIBA LabRAM HR Evolution microscope confocal laser Raman spectrometer was used to detect *in-situ* temperature-varying Raman modes in the VO₂ epitaxial films. A laser with a wavelength of 532 nm was selected, and the laser power was set to approximately 0.25 mW. The objective lens was a magnification of ×50, and the unit data acquisition time was 20 s. The rate of temperature change was approximately 10°C/min during the heating process, and the cooling process naturally decreased to room temperature. The temperature was maintained for 4 min after it reached a fixed point to maintain stability and consistency.

RESULTS AND DISCUSSION

Phase Structure and ϕ -Scans of VO₂/Al₂O₃ Films

Figures 1A,B show the crystal structure of VO₂. In general, the SPT in VO₂ refers to the process of the monoclinic phase (M1) transforming into the tetragonal phase (R) (Mott, 1990; Shi and Chen, 2018). When the temperature is below the phase transition temperature, VO₂ is in a monoclinic phase. In this state, the V atoms in the crystal spontaneously dimerize along the a_M -axis, forming a twisted zig-zag chain, as shown in Figure 1A. Because



the V–V atoms have two different distances, resulting in the localization of the *d*-orbital electrons in the V–V dimer, they exhibit the properties of an insulating state (Shimizu et al., 2020). In contrast, in the R phase, as shown in **Figure 1B**, the V–V atom chain along the *c_R*-axis direction is not paired, leading to the disappearance of V–V dimerization and the emergence of a linear chain (Morrison et al., 2014). As a consequence, the MIT occurs with a resistivity change of nearly three to four orders of magnitude as shown in **Figure 1D**. Moreover, the resistance vs. temperature curve shows a reversible hysteresis with a critical temperature of approximately 62.9 and 73.6°C in the heating and cooling process (see details in **Supplementary Figure S1** in Supplementary Materials).

To verify the growth direction of the VO₂ thin film on the (0001) surface of the Al₂O₃ substrate, we first performed a normal θ -2 θ line scan of XRD at room temperature and determined the VO₂ [010] along the out-of-plane direction (see the following results), which is consistent with previous reports (Yang et al., 2015a; Muramoto et al., 2020). Second, we confirmed the in-plane growth orientation of the VO₂/Al₂O₃ thin film using high-resolution XRD at room temperature. **Figure 1C** shows the ϕ -scan results for the VO₂ (011) and (220) and Al₂O₃ (208) reflections. The positions of the VO₂ (011) and (220) peaks were at the same azimuthal position and separated by 60° (Nag et al., 2011). Furthermore, three-fold symmetry of the Al₂O₃ (208) reflection was also observed owing to the triple

symmetry of the (0001) surface with respect to the *c*-axis of Al₂O₃ (Zhang et al., 1999; Yang et al., 2011). In addition to a two-fold symmetry with respect to the *b*-axis in monoclinic VO₂, six peaks in both the VO₂ (011) and (220) ϕ -scans were observed, indicating an emergence of the structural twinned domain. Upon close inspection, the individual VO₂ (011) peak was found to split into two peaks, that is, a doublet, which was caused by a β -angle mismatch between VO₂ and the Al₂O₃ substrate. Moreover, the individual VO₂ (220) peak revealed that each of the main peaks was surrounded by two smaller satellite peaks with a triplet feature, which may be caused by the V–V zig-zag chain deviating from the monoclinic *a_M*-axis (Zhao et al., 2012; Fan et al., 2013; Yang et al., 2018a).

Characterizing the Lattice Constants and Mismatch Angle

To explore the SPT of VO₂ thin films across the MIT, we employed *in-situ* variable-temperature high-resolution XRD at the BL14B1 beamline of the SSRF. **Figures 2A,B** show the local θ -2 θ scans of epitaxial VO₂ films on sapphire substrates during the heating and cooling processes, respectively, in the temperature range 30–90°C. Overall, the Al₂O₃ (0006) peak barely moved during the entire heating and cooling processes, strongly indicating that thermal effect during heating and cooling process can be ignored in discussing SPT of the VO₂ thin

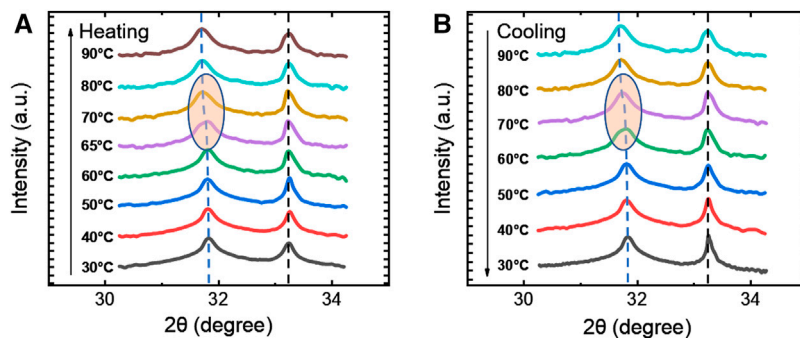


FIGURE 2 | Local XRD θ - 2θ scan patterns of VO₂/Al₂O₃ during the (A) heating and (B) cooling processes.

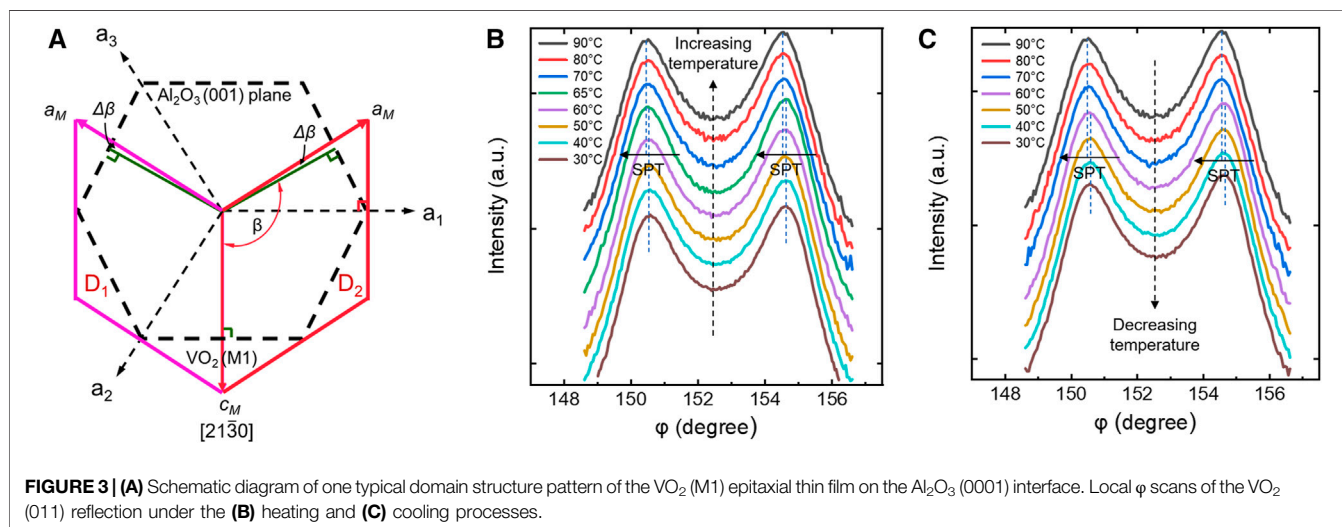
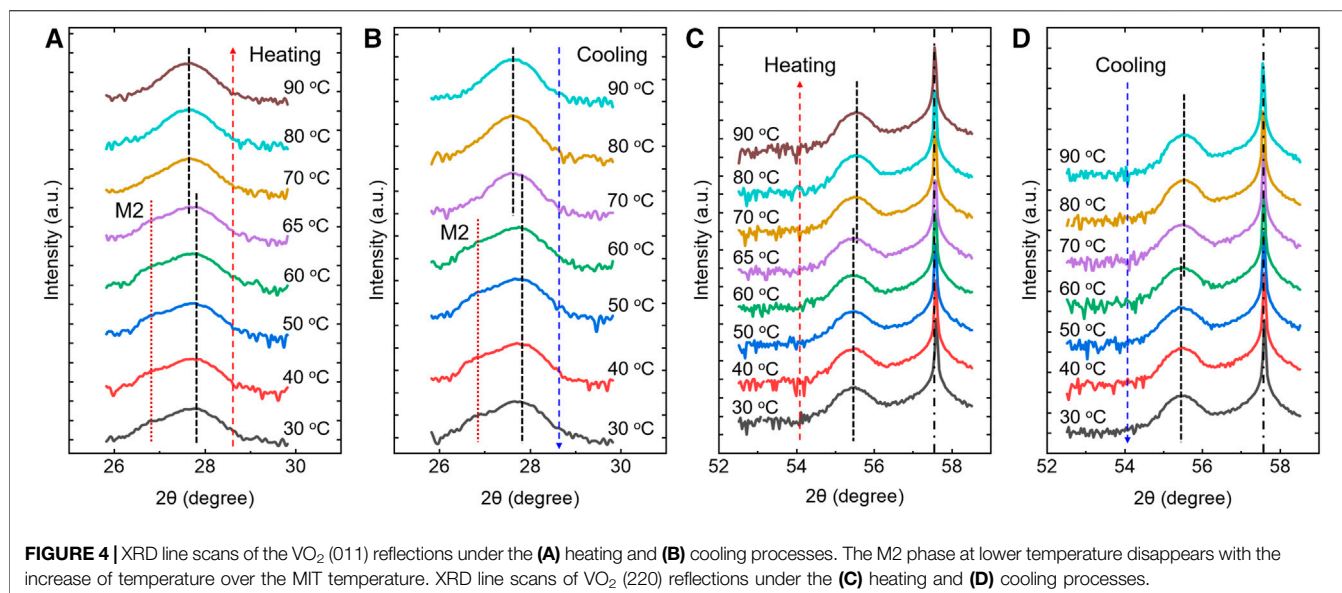


FIGURE 3 | (A) Schematic diagram of one typical domain structure pattern of the VO₂ (M1) epitaxial thin film on the Al₂O₃ (0001) interface. Local ϕ scans of the VO₂ (011) reflection under the (B) heating and (C) cooling processes.

films. Whereas the VO₂ (020) reflection moved to a lower angle during the heating process and back to a higher angle during the cooling process, indicating a reversible SPT across the MIT. The diffraction peak of VO₂ (020) was located at approximately 31.83° at 30°C during the heating and cooling processes. In particular, the 2θ shift of the VO₂ (020) reflection was more obvious in the temperature range of approximately 60–70°C, as indicated by the ellipse in **Figures 2A,B**, then reached approximately 31.72 at 90°C, resulting in elongating of the lattice space of the VO₂ (020) plane. Because the b -axis is perpendicular to the VO₂ (020) plane, the plane space directly reflects the lattice constant b (Yang et al., 2018b). Consequently, the lattice constant b should be increased upon heating, which is consistent with the occurrence of SPT, as reported in previous studies (Park et al., 2013).

By combining the above structural information, we can infer the possible structural domain configuration of the VO₂ thin film on the (0001)-Al₂O₃ substrate, as shown in **Figure 3A**. The Al₂O₃ (0001) surface exhibited a hexagonal structure, and the VO₂ film was epitaxially grown on it with the b -axis along the out-of-plane direction. Therefore, the a -axis and c -axis of the VO₂ film matched the (0001) plane of the Al₂O₃ substrate. Based on

Figures 1C, 2A,B, two types of domain configurations were derived, as shown in **Figure 3A**. The c_M -axis was determined along the Al₂O₃ [21 $\bar{3}$ 0] direction, and the a_M -axis had an angle mismatch $\Delta\beta$ with respect to the vertical line, as marked in green for easy identification. One can easily derive the other two configurations of structural domain using triple symmetry operation with respect to the c -axis of Al₂O₃ as reported in ref. 38. The offset angle, $\Delta\beta$, reflects the angular mismatch between the VO₂ (020) and Al₂O₃ (0001) planes (Yang et al., 2010; Yang et al., 2015b), which can be quantitatively obtained from ϕ -scans of the VO₂ (011) reflections. Subsequently, we performed *in-situ* temperature-variable local ϕ -scans of the nonsymmetric VO₂ (011) reflection, as shown in **Figures 3B,C** (Chen et al., 2010). The two azimuthal angles of the VO₂ (011) doublet both moved to a lower angle and clearly decreased under the heating process in the temperature range 60–70°C, which strongly indicates the appearance of the SPT as shown in **Figures 3B,C**. Herein the azimuthal angle difference of the doublet was twice the mismatch angle $\Delta\beta$. By measuring the angle $2\Delta\beta$ in the VO₂ (011) doublet, an important lattice parameter, β ($=120^\circ + \Delta\beta$), between the a -axis and c -axis can be obtained across the MIT (Fan et al., 2013).



Next, we quantitatively determined the other two lattice parameters a and c . The remaining two nonsymmetric reflections, that is, the VO₂ (011) and (220) diffraction peaks, were selected. θ - 2θ line scans were performed to obtain the temperature-dependent reflection shift using in-house high-resolution XRD with Cu $K\alpha_1$ radiation. In the XRD line scans of the VO₂ (011) reflection, as shown in **Figures 4A,B**, when the VO₂ thin film was in the low-temperature monoclinic phase during the heating process, 2θ was 27.87°; with an increase in temperature, the peak position of 2θ gradually shifted to a lower angle position. Moreover, the change was more obvious in the temperature range 65–70°C; the peak position changed to 27.67° at 90°C. The VO₂ (011) reflection shifted back during the cooling process. It is worth mentioning that the monoclinic M2 phase should exist near the interface at relatively lower temperature due to the substrate constraints (Hu et al., 2010). Similarly, in the XRD line scans of the VO₂ (220) crystal plane, as shown in **Figures 4C,D**, the peak position of VO₂ (220) shifted to a higher angle position in the heating process and back in the cooling process. Note that, regardless of the heating or cooling process, the peak position of the Al₂O₃ (116) reflection at $2\theta = 57.56^\circ$ remained unchanged, which is a good indicator for the SPT in VO₂ thin films.

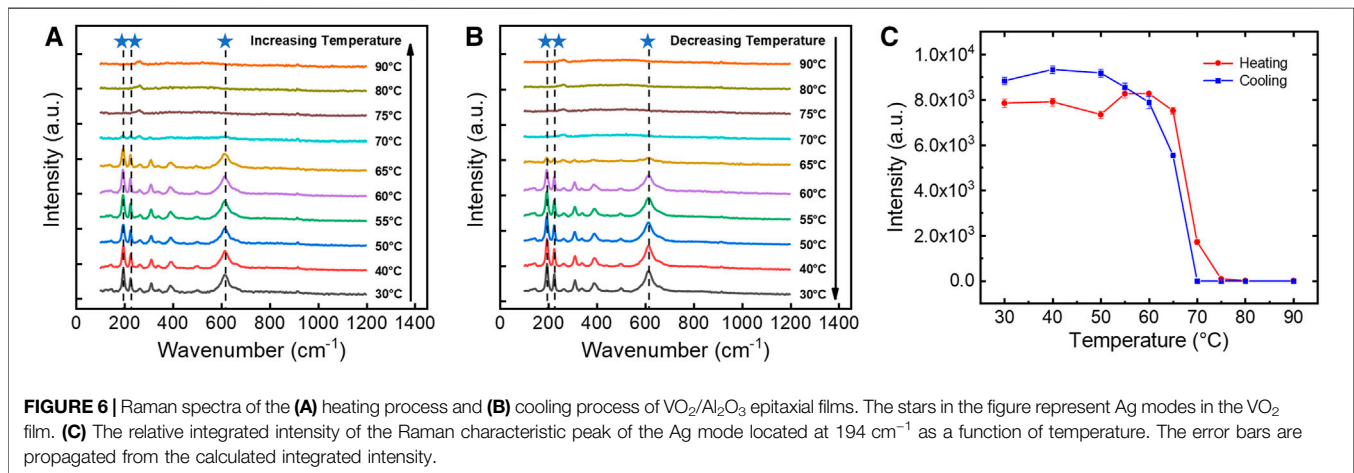
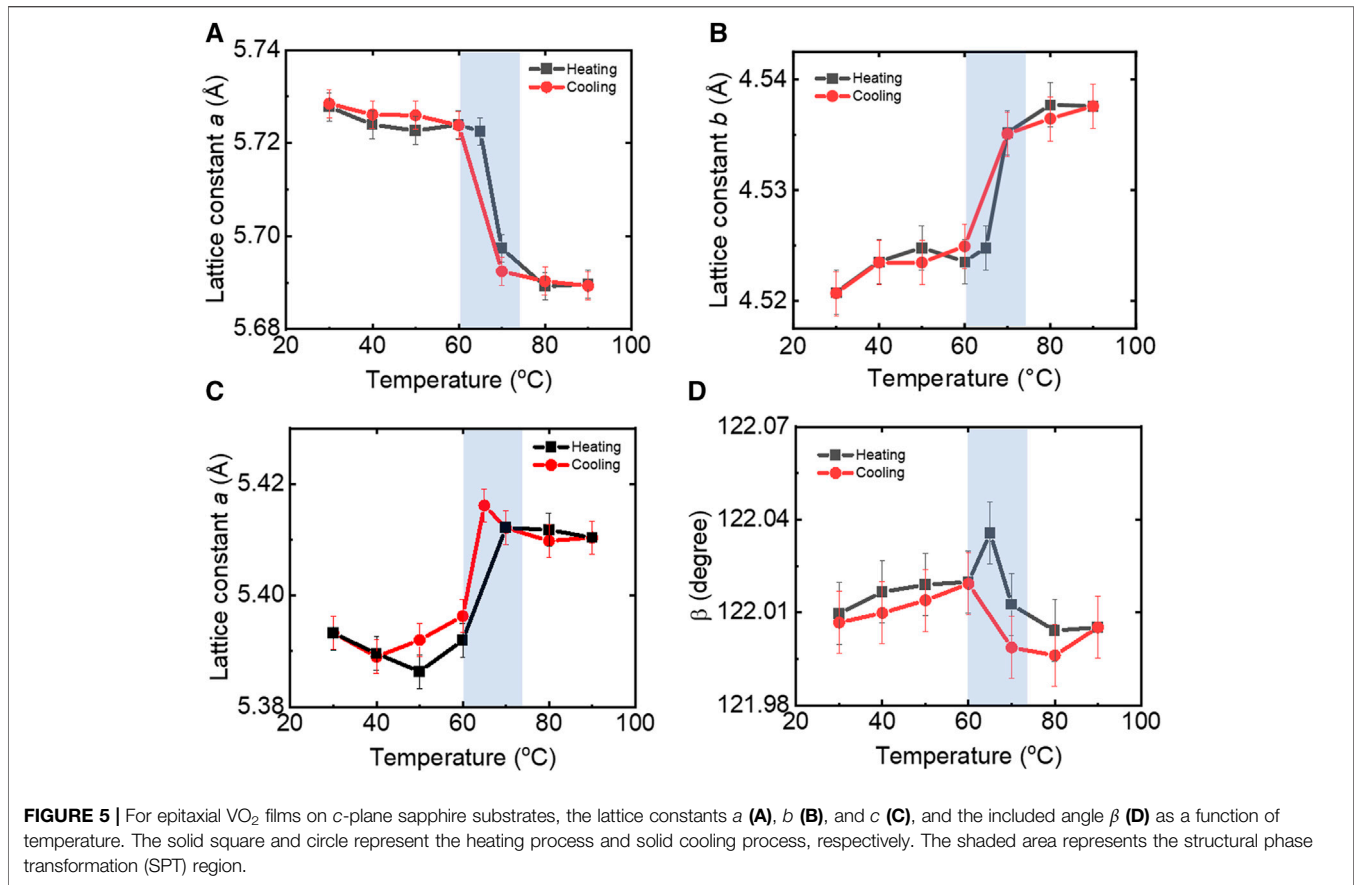
Using local θ - 2θ scans of the (020) peaks of VO₂, the out-of-plane lattice parameter b can be obtained using the Bragg formula: $2b \sin \theta = \lambda$. Similarly, we can obtain the interplanar spacing $d_{(hkl)}$ of the VO₂ (011) and (220) crystal planes under *in-situ* variable temperatures. The lattice parameters can then be calculated in the notation of the monoclinic crystal structure according to the following interplanar spacing $d_{(hkl)}$ formula:

$$\frac{1}{d_{(hkl)}^2} = \left\{ \frac{h^2}{a^2} + \frac{k^2 \sin^2 \beta}{b^2} + \frac{l^2}{c^2} - \frac{2hl \cos \beta}{ac} \right\} / \sin^2 \beta \quad (1)$$

Where β is the mismatch angle between the a - and c -axis in the VO₂ crystal structure. This can be obtained from **Figures 3B,C**, as

mentioned above (Longo et al., 1970). Next, we can simultaneously calculate the lattice parameters a and c during the heating and cooling processes.

The lattice constants a , b , and c , and the β angle during the heating and cooling processes are summarized in **Figure 5**. Overall, the lattice parameters of the monoclinic VO₂ film at a low temperature (~30°C) were $a = 5.723 \text{ \AA}$, $b = 4.521 \text{ \AA}$, $c = 5.393 \text{ \AA}$, and the included angle $\beta = 122.01^\circ$. Comparing with the bulk lattice constants a , b , and c approximately 5.755, 4.525, and 5.383 Å (Rakotoniaina et al., 1993), the out-of-plane strain seems relaxed. Moreover, the tensile strain along the c_M -axis indeed establishes, which should be due to the thermal expansion mismatch between the VO₂ thin film and Al₂O₃ substrate (Théry et al., 2016). However, the in-plane strain along the a_M -axis is compressive, which may be responsible for the volume conservation of VO₂ unit cell. Therefore, herein the biaxial anisotropic strain is developed and does not seem to affect the MIT temperature as shown **Figure 1D**. This case is different from the biaxial tensile strain in Ref. 49. As increasing temperature, the lattice parameters of the high-temperature tetragonal VO₂ film were $a = 5.689 \text{ \AA}$, $b = 4.538 \text{ \AA}$, $c = 5.411 \text{ \AA}$, and $\beta = 122.00^\circ$. It is mentionable that the determination of the lattice constant in the high-temperature rutile phase is still in the framework of the monoclinic symmetry for better illustrating the lattice change across the MIT, the same as the low-temperature monoclinic phase. Interestingly, the lattice parameter c in the (010)-VO₂/(0001)-Al₂O₃ epitaxial thin films in this study increased during the heating process, whereas the lattice parameters a and c of bulk VO₂ both decreased during the transition from the monoclinic to tetragonal phase (Rakotoniaina et al., 1993). Such a distinct change trend could be attributed to the substrate-induced thermal strain in the (010)-VO₂/(0001)-Al₂O₃ epitaxial thin film (Yang et al., 2015a; Théry et al., 2016; Yang et al., 2018a), which will be further studied in the future. Moreover, as indicated in pale blue in **Figure 5**, sharp changes in the lattice



constants *a*, *b*, and *c*, and angle β were observed, indicating the occurrence of the SPT in the heating and cooling processes (Park et al., 2013; McGee et al., 2018). Combined with the transport properties shown in Figure 1D and Supplementary Figure S1, the emergence of SPT is a natural concomitant of the MIT in VO₂/Al₂O₃ thin films (Zhang et al., 2017). In particular, as shown in Figure 5D, a clear increase in the angle β was observed during the heating process, which could be related to the disappearance of the M2 phase in the vicinity of the MIT

(Hu et al., 2010; Pellegrino et al., 2012). This conjecture is evidenced in Figures 4A,B.

Verifying SPT Using Raman Spectroscopy

To confirm the above SPT, *in-situ* variable temperature Raman characterization was carried out, as shown in Figures 6A,B. First, overall, the temperature-variable Raman spectra were reversible in the heating and cooling processes. Additionally, there was significant hysteresis in the temperature range of approximately

65–70°C. Second, during the heating process, the characteristic Raman peak at 70°C, shown in **Figure 6A**, disappeared, indicating SPT from the M1 to R phase. The SPT temperature was close to the MIT temperature. As the temperature continued to increase, the peaks in the Raman spectrum gradually became weaker and eventually disappeared. This corresponds to the first-order phase transition of the crystal structure of VO₂ from a low-symmetry monoclinic phase to a high-symmetry rutile phase. Conversely, as shown in **Figure 6B**, during the cooling process, the peaks in the Raman spectrum gradually recovered and finally agreed with the typical VO₂ Raman spectrum of the low-temperature M1 phase. This corresponds to the SPT of VO₂ thin films from a high-symmetry rutile phase to a low-symmetry monoclinic phase (Pan et al., 2004). Moreover, we investigated the three characteristic peaks in the Raman spectra of the VO₂/Al₂O₃ epitaxial film in detail, which were located at 194, 226, and 616 cm⁻¹ (Marini et al., 2008; Yu et al., 2013; Chang et al., 2014). These were assigned to the Ag vibrational modes associated with V–V dimerization, which are indicated by stars in **Figures 6A,B**. The other weaker Ag vibrational modes were located at approximately 145, 311, 390 and 500 cm⁻¹. The peaks reflecting the V–O Bg vibrational mode were located at approximately 263, 342, 447 cm⁻¹ (Ji et al., 2014). These distinct vibrational peaks indicate that the VO₂ epitaxial film is essentially insulating with a monoclinic phase (M1). Moreover, the sharp and strong intensity of the Ag mode indicates that the VO₂/Al₂O₃ epitaxial film has a good crystal quality, which is consistent with the above XRD characterization results.

Following this, we performed Gaussian fitting on the corresponding characteristic peak at 194 cm⁻¹ and obtained the relationship between the relative integral intensity of this peak and the *in-situ* variable temperature, as shown in **Figure 6C**. The relative integral intensities of the characteristic peaks in the other two representative Ag modes as a function of temperature are shown in **Supplementary Figure S2** of the Supplementary Material. The integral intensity of the characteristic Ag mode exhibited an abrupt change in the temperature region of approximately 65–70°C in both the heating and cooling processes, which verifies that SPT occurs near the MIT in VO₂ thin films. Additionally, at high temperatures, the relative integrated intensity of the Ag mode almost decreased to zero, indicating that the monoclinic insulating phase no longer existed. It is mentionable that a slight enhancement of the relative integrated intensity as cycling back to room temperature was probably attributed to a reduction of light absorption, owing to decreasing pressure of the sample chamber. Moreover, at high temperatures, the Raman spectra exhibited almost no characteristic peaks, which is a typical feature of the tetragonal metallic phase (Ji et al., 2014). These results strongly demonstrate that reversible SPT occurs concomitantly across the MIT in (010)-VO₂/(0001)-Al₂O₃ thin films from the perspective of temperature parameter space.

CONCLUSION

In summary, we successfully grew VO₂ epitaxial films on Al₂O₃ (0001) substrates using reactive magnetron sputtering. The VO₂ epitaxial thin films exhibited a clear MIT behavior in the temperature range of approximately 65–70°C. A remarkable

feature is the sharp change in the lattice parameters *a*, *b*, and *c* from 5.723, 4.521, and 5.393 Å at low temperatures to 5.689, 4.538, and 5.411 Å, at high temperatures, respectively. Additionally, the included angle β increased from 122.01° at 30°C then sharply decreased at the MIT temperature, implying the occurrence of SPT. By combining quantitative structure characterizations and transport property measurements, the co-occurrence of the SPT and MIT was experimentally observed from the perspective of temperature parameter space in the (010)-VO₂/(0001)-Al₂O₃ thin films, which was further confirmed by Raman spectroscopy. Moreover, the SPT in such thin-film systems is distinct from its bulk counterparts (for example, single-crystal, polycrystalline, or nanostructured samples). This study provides a general strategy for re-examining the SPT in different VO₂ systems.

DATA AVAILABILITY STATEMENT

The raw data supporting the conclusions of this article will be made available by the authors, without undue reservation.

AUTHOR CONTRIBUTIONS

YY and HZ conceived this work and designed the experiments. CW and WH optimized the VO₂ thin films growth conditions and performed transport property characterizations. YL and SW fabricated the thin films. YL, WG, and MC performed Raman characterization. YG, XZ, XL, XG, and YY carried out XRD characterization. CW performed experimental data analysis and gave a very valuable discussion. YL and YY wrote the paper. All the authors have revised it and gave a last approval to this work.

FUNDING

This research was mainly supported by the Open Foundation of the University of Science and Technology of China (KF2020002) and partially funded by the National Natural Science Foundation of China (52072102, 11804324, and 12074357) and the National Key Research and Development Program of China (2017YFA0205004).

ACKNOWLEDGMENTS

HZ is especially grateful for the support from the Chinese Academy of Sciences Pioneer Hundred Talents Program. The authors highly appreciate the beamlines BL07W, BL10B, BL11U, and BL12B- α at the National Synchrotron Radiation Laboratory (NSRL) for the preliminary characterization of the electronic structure.

SUPPLEMENTARY MATERIAL

The Supplementary Material for this article can be found online at: <https://www.frontiersin.org/articles/10.3389/fmats.2022.866468/full#supplementary-material>

REFERENCES

- Aetukuri, N. B., Gray, A. X., Drouard, M., Cossale, M., Gao, L., Reid, A. H., et al. (2013). Control of the Metal-Insulator Transition in Vanadium Dioxide by Modifying Orbital Occupancy. *Nat. Phys.* 9, 661–666. doi:10.1038/nphys2733
- Baum, P., Yang, D.-S., and Zewail, A. H. (2007). 4D Visualization of Transitional Structures in Phase Transformations by Electron Diffraction. *Science* 318, 788–792. doi:10.1126/science.1147724
- Cao, J., Ertekin, E., Srinivasan, V., Fan, W., Huang, S., Zheng, H., et al. (2009). Strain Engineering and One-Dimensional Organization of Metal-Insulator Domains in Single-crystal Vanadium Dioxide Beams. *Nat. Nanotech* 4, 732–737. doi:10.1038/nnano.2009.266
- Chang, S.-J., Park, J. B., Lee, G., Kim, H. J., Lee, J.-B., Bae, T.-S., et al. (2014). *In Situ* probing of Doping- and Stress-Mediated Phase Transitions in a Single-Crystalline VO₂ Nanobeam by Spatially Resolved Raman Spectroscopy. *Nanoscale* 6, 8068–8074. doi:10.1039/c4nr01118j
- Chen, S., Ma, H., Yi, X., Xiong, T., Wang, H., and Ke, C. (2004). Smart VO₂ Thin Film for protection of Sensitive Infrared Detectors from strong Laser Radiation. *Sensors Actuators A: Phys.* 115, 28–31. doi:10.1016/j.sna.2004.03.018
- Chen, C., Zhu, Y., Zhao, Y., Lee, J. H., Wang, H., Bernussi, A., et al. (2010). VO₂ Multidomain Heteroepitaxial Growth and Terahertz Transmission Modulation. *Appl. Phys. Lett.* 97, 211905. doi:10.1063/1.3519361
- Cocker, T. L., Titova, L. V., Fourmaux, S., Holloway, G., Bandulet, H.-C., Brassard, D., et al. (2012). Phase Diagram of the Ultrafast Photoinduced Insulator-Metal Transition in Vanadium Dioxide. *Phys. Rev. B* 85, 155120. doi:10.1103/physrevb.85.155120
- Driscoll, T., Kim, H.-T., Chae, B.-G., Kim, B.-J., Lee, Y.-W., Jokerst, N. M., et al. (2009). Memory Metamaterials. *Science* 325, 1518–1521. doi:10.1126/science.1176580
- Fan, L. L., Wu, Y. F., Si, C., Zou, C. W., Qi, Z. M., Li, L. B., et al. (2012). Oxygen Pressure Dependent VO₂ crystal Film Preparation and the Interfacial Epitaxial Growth Study. *Thin Solid Films* 520, 6124–6129. doi:10.1016/j.tsf.2012.05.086
- Fan, L. L., Wu, Y. F., Si, C., Pan, G. Q., Zou, C. W., and Wu, Z. Y. (2013). Synchrotron Radiation Study of VO₂ crystal Film Epitaxial Growth on Sapphire Substrate with Intrinsic Multi-Domains. *Appl. Phys. Lett.* 102, 011604. doi:10.1063/1.4775580
- Hu, B., Ding, Y., Chen, W., Kulkarni, D., Shen, Y., Tsukruk, V. V., et al. (2010). External-Strain Induced Insulating Phase Transition in VO₂ Nanobeam and its Application as Flexible Strain Sensor. *Adv. Mater.* 22, 5134–5139. doi:10.1002/adma.201002868
- Huang, W.-x., Yin, X.-g., Huang, C.-p., Wang, Q.-j., Miao, T.-f., and Zhu, Y.-y. (2010). Optical Switching of a Metamaterial by Temperature Controlling. *Appl. Phys. Lett.* 96, 261908. doi:10.1063/1.3458706
- Imada, M., Fujimori, A., and Tokura, Y. (1998). Metal-Insulator Transitions. *Rev. Mod. Phys.* 70, 1039–1263. doi:10.1103/revmodphys.70.1039
- Jeong, J., Aetukuri, N., Graf, T., Schladt, T. D., Samant, M. G., and Parkin, S. S. P. (2013). Suppression of Metal-Insulator Transition in VO₂ by Electric Field-Induced Oxygen Vacancy Formation. *Science* 339, 1402–1405. doi:10.1126/science.1230512
- Ji, Y., Zhang, Y., Gao, M., Yuan, Z., Xia, Y., Jin, C., et al. (2014). Role of Microstructures on the M1-M2 Phase Transition in Epitaxial VO₂ Thin Films. *Sci. Rep.* 4, 4854. doi:10.1038/srep04854
- Wang, K., Cheng, C., Cardona, E., Guan, J., Liu, K., and Wu, J. (2013). Performance Limits of Microactuation with Vanadium Dioxide as a Solid Engine. *ACS Nano* 7, 2266–2272. doi:10.1021/nn305419e
- Lee, S., Meyer, T. L., Sohn, C., Lee, D., Nichols, J., Lee, D., et al. (2015). Electronic Structure and Insulating gap in Epitaxial VO₂ Polymorphs. *APL Mater.* 3 (12), 126109. doi:10.1063/1.4939004
- Lee, S., Hippalgaonkar, K., Yang, F., Hong, J., Ko, C., Suh, J., et al. (2017). Anomalous Low Electronic thermal Conductivity in Metallic Vanadium Dioxide. *Science* 355, 371–374. doi:10.1126/science.aag0410
- Lee, D., Chung, B., Shi, Y., Kim, G.-Y., Campbell, N., Xue, F., et al. (2018). Isostructural Metal-Insulator Transition in VO₂. *Science* 362, 1037–1040. doi:10.1126/science.aam9189
- Liu, M., Sternbach, A. J., Wagner, M., Slusar, T. V., Kong, T., Bud'ko, S. L., et al. (2015). Phase Transition in Bulk Single Crystals and Thin Films of VO₂ by Nanoscale Infrared Spectroscopy and Imaging. *Phys. Rev. B* 91, 245155. doi:10.1103/physrevb.91.245155
- Longo, J. M., Kierkegaard, P., Ballhausen, C. J., Ragnarsson, U., Rasmussen, S. E., Sunde, E., et al. (1970). A Refinement of the Structure of VO₂. *Acta Chem. Scand.* 24, 420–426. doi:10.3891/acta.chem.scand.24-0420
- Lysenko, S., Rua, A. J., Vikhain, V., Jimenez, J., Fernandez, F., and Liu, H. (2006). Light-induced Ultrafast Phase Transitions in VO₂ Thin Film. *Appl. Surf. Sci.* 252, 5512–5515. doi:10.1016/j.apsusc.2005.12.137
- Marini, C., Arcangeletti, E., Di Castro, D., Baldassare, L., Perucchi, A., Lupi, S., et al. (2008). Optical Properties of V_{1-x}Cr_xO₂ Compounds under High Pressure. *Phys. Rev. B* 77, 235111. doi:10.1103/physrevb.77.235111
- McGee, R., Goswami, A., Pal, S., Schofield, K., Bukhari, S. A. M., and Thundat, T. (2018). Sharpness and Intensity Modulation of the Metal-Insulator Transition in Ultrathin VO₂ Films by Interfacial Structure Manipulation. *Phys. Rev. Mater.* 2, 034605. doi:10.1103/physrevmaterials.2.034605
- Morin, F. J. (1959). Oxides Which Show a Metal-To-Insulator Transition at the Neel Temperature. *Phys. Rev. Lett.* 3, 34–36. doi:10.1103/physrevlett.3.34
- Morrison, V. R., Chatelain, R. P., Tiwari, K. L., Hendaoui, A., Bruhács, A., Chaker, M., et al. (2014). A Photoinduced Metal-like Phase of Monoclinic VO₂ Revealed by Ultrafast Electron Diffraction. *Science* 346, 445–448. doi:10.1126/science.1253779
- Mott, N. F. (1990). *Metal-insulator Transitions*. 2nd ed. London: CRC Press.
- Muramoto, K., Takahashi, Y., Terakado, N., Yamazaki, Y., Suzuki, S., and Fujiwara, T. (2020). Fabrication of VO₂-Dispersed Glass in B₂O₃-P₂O₅-V₂O₅ System and its Thermal Property. *Front. Mater.* 7, 5. doi:10.3389/fmats.2020.00005
- Nag, J., Payzant, E. A., More, K. L., and Haglund, R. F. (2011). Enhanced Performance of Room-Temperature-Grown Epitaxial Thin Films of Vanadium Dioxide. *Appl. Phys. Lett.* 98, 251916. doi:10.1063/1.3600333
- Nakajima, M., Takubo, N., Hiroi, Z., Ueda, Y., and Suemoto, T. (2008). Photoinduced Metallic State in Proved by the Terahertz Pump-Probe Spectroscopy. *Appl. Phys. Lett.* 92, 011907. doi:10.1063/1.2830664
- Nakano, M., Shibuya, K., Okuyama, K., Hatano, T., Ono, S., Kawasaki, M., et al. (2012). Collective Bulk Carrier Delocalization Driven by Electrostatic Surface Charge Accumulation. *Nature* 487, 459–462. doi:10.1038/nature11296
- Wang, N., Huang, Y., Magdassi, S., Mandler, D., Liu, H., and Long, Y. (2013). Formation of VO₂ Zero-Dimensional/nanoporous Layers with Large Supercooling Effects and Enhanced Thermochemical Properties. *RSC Adv.* 3, 7124. doi:10.1039/c3ra40370j
- Pan, M., Liu, J., Zhong, H., Wang, S., Li, Z.-f., Chen, X., et al. (2004). Raman Study of the Phase Transition in VO₂ Thin Films. *J. Cryst. Growth* 268, 178–183. doi:10.1016/j.jcrysgro.2004.05.005
- Park, J., Oh, I. H., Lee, E., Lee, K. W., Lee, C. E., Song, K., et al. (2007). Structure and Magnetism in VO₂ Nanorods. *Appl. Phys. Lett.* 91, 153112. doi:10.1063/1.2798587
- Park, J. H., Coy, J. M., Kasirga, T. S., Huang, C., Fei, Z., Hunter, S., et al. (2013). Measurement of a Solid-State Triple point at the Metal-Insulator Transition in VO₂. *Nature* 500, 431–434. doi:10.1038/nature12425
- Pellegrino, L., Manca, N., Kanki, T., Tanaka, H., Biasotti, M., Bellingeri, E., et al. (2012). Multistate Memory Devices Based on Free-Standing VO₂/TiO₂ Microstructures Driven by Joule Self-Heating. *Adv. Mater.* 24, 2929–2934. doi:10.1002/adma.201104669
- Rakotoniaina, J. C., Mokrani-Tamellin, R., Gavarrí, J. R., Vacquier, G., Casalot, A., and Calvarin, G. (1993). The Thermochemical Vanadium Dioxide. I. Role of Stresses and Substitution on Switching Properties. *J. Solid State. Chem.* 103, 81–94. doi:10.1006/jssc.1993.1081
- Sharma, Y., Balachandran, J., Sohn, C., Krogel, J. T., Ganesh, P., Collins, L., et al. (2018). Nanoscale Control of Oxygen Defects and Metal-Insulator Transition in Epitaxial Vanadium Dioxides. *ACS Nano* 12, 7159–7166. doi:10.1021/acsnano.8b03031
- Shi, Y., and Chen, L. Q. (2018). Phase-field Model of Insulator-To-Metal Transition in VO₂ under an Electric Field. *Phys. Rev. Mater.* 2, 053803. doi:10.1103/physrevmaterials.2.053803
- Shimizu, Y., Jin-no, T., Iwase, F., Itoh, M., and Ueda, Y. (2020). Occupation Switching of *D* Orbitals in Vanadium Dioxide Probed via Hyperfine Interactions. *Phys. Rev. B* 101, 245123. doi:10.1103/physrevb.101.245123
- Stefanovich, G., Pergament, A., and Stefanovich, D. (2000). Electrical Switching and Mott Transition in VO₂. *J. Phys. Condens. Matter* 12, 8837–8845. doi:10.1088/0953-8984/12/41/310

- Théry, V., Boule, A., Crunteanu, A., Orlianges, J. C., Beaumont, A., Mayet, R., et al. (2016). Role of thermal Strain in the Metal-Insulator and Structural Phase Transition of Epitaxial VO₂ Films. *Phys. Rev. B* 93, 184106. doi:10.1103/physrevb.93.184106
- Wall, S., Yang, S., Vidas, L., Chollet, M., Glownia, J. M., Kozina, M., et al. (2018). Ultrafast Disorder of Vanadium Dimers in Photoexcited VO₂. *Science* 362, 572–576. doi:10.1126/science.aau3873
- Yang, T.-H., Jin, C., Aggarwal, R., Narayan, R. J., and Narayan, J. (2010). On Growth of Epitaxial Vanadium Oxide Thin Film on Sapphire (0001). *J. Mater. Res.* 25, 422–426. doi:10.1557/jmr.2010.0059
- Yang, T.-H., Mal, S., Jin, C., Narayan, R. J., and Narayan, J. (2011). Epitaxial VO₂/Cr₂O₃/sapphire Heterostructure for Multifunctional Applications. *Appl. Phys. Lett.* 98, 022105. doi:10.1063/1.3541649
- Yang, M., Yang, Y., Hong, B., Wang, L., Luo, Z., Li, X., et al. (2015a). Surface-growth-mode-induced Strain Effects on the Metal-Insulator Transition in Epitaxial Vanadium Dioxide Thin Films. *RSC Adv.* 5, 80122–80128. doi:10.1039/c5ra13490k
- Yang, M., Yang, Y., Hong, B., Huang, H., Hu, S., Dong, Y., et al. (2015b). Resistance Switching of Epitaxial VO₂/Al₂O₃ Heterostructure at Room Temperature Induced by Organic Liquids. *AIP Adv.* 5, 037114. doi:10.1063/1.4914915
- Yang, Y., Wang, L., Huang, H., Kang, C., Zong, H., Zou, C., et al. (2018a). Controlling Metal-Insulator Transition in (010)-VO₂/(0001)-Al₂O₃ Epitaxial Thin Film through Surface Morphological Engineering. *Ceramics Int.* 44, 3348–3355. doi:10.1016/j.ceramint.2017.11.121
- Yang, Y., Yao, Y., Zhang, B., Lin, H., Luo, Z., Gao, C., et al. (2018b). Investigating Metal-Insulator Transition and Structural Phase Transformation in the (010)-VO₂/(001)-YSZ Epitaxial Thin Films. *Materials* 11, 1713. doi:10.3390/ma11091713
- Yao, T., Zhang, X., Sun, Z., Liu, S., Huang, Y., Xie, Y., et al. (2010). Understanding the Nature of the Kinetic Process in a VO₂ Metal-Insulator Transition. *Phys. Rev. Lett.* 105, 226405. doi:10.1103/physrevlett.105.226405
- Yu, Q., Li, W., Liang, J., Duan, Z., Hu, Z., Liu, J., et al. (2013). Oxygen Pressure Manipulations on the Metal-Insulator Transition Characteristics of Highly (0 1 1)-oriented Vanadium Dioxide Films Grown by Magnetron Sputtering. *J. Phys. D: Appl. Phys.* 46, 055310. doi:10.1088/0022-3727/46/5/055310
- Yu, S., Wang, S., Lu, M., and Zuo, L. (2017). A Metal-Insulator Transition Study of VO₂ Thin Films Grown on Sapphire Substrates. *J. Appl. Phys.* 122, 235102. doi:10.1063/1.4997437
- Zhang, Z. J., Narumi, K., Naramoto, H., Wu, Z. P., Yamamoto, S., Miyashita, A., et al. (1999). A Crystalline Hydrogenated Carbon Film Obtained by Plasma Enhanced Chemical Vapor Deposition. *J. Appl. Phys.* 86, 1317–1321. doi:10.1063/1.370888
- Zhang, Z., Zuo, F., Wan, C., Dutta, A., Kim, J., Rensberg, J., et al. (2017). Evolution of Metallicity in Vanadium Dioxide by Creation of Oxygen Vacancies. *Phys. Rev. Appl.* 7, 034008. doi:10.1103/physrevapplied.7.034008
- Zhang, C., Koughia, C., Güneş, O., Luo, J., Hossain, N., Li, Y., et al. (2020). Synthesis, Structure and Optical Properties of High-Quality VO₂ Thin Films Grown on Silicon, Quartz and Sapphire Substrates by High Temperature Magnetron Sputtering: Properties through the Transition Temperature. *J. Alloys Compd.* 848, 156323. doi:10.1016/j.jallcom.2020.156323
- Zhao, Y., Hwan Lee, J., Zhu, Y., Nazari, M., Chen, C., Wang, H., et al. (2012). Structural, Electrical, and Terahertz Transmission Properties of VO₂ Thin Films Grown on C-, R-, and M-Plane Sapphire Substrates. *J. Appl. Phys.* 111, 053533. doi:10.1063/1.3692391
- Zhou, J., Gao, Y., Zhang, Z., Luo, H., Cao, C., Chen, Z., et al. (2013). VO₂ Thermochromic Smart Window for Energy Savings and Generation. *Sci. Rep.* 3, 3029. doi:10.1038/srep03029

Conflict of Interest: The authors declare that the research was conducted in the absence of any commercial or financial relationships that could be construed as a potential conflict of interest.

Publisher's Note: All claims expressed in this article are solely those of the authors and do not necessarily represent those of their affiliated organizations, or those of the publisher, the editors and the reviewers. Any product that may be evaluated in this article, or claim that may be made by its manufacturer, is not guaranteed or endorsed by the publisher.

Copyright © 2022 Liu, Wang, Huang, Wang, Qiu, Ge, Chen, Zhang, Gu, Zhang, Li, Gao and Yang. This is an open-access article distributed under the terms of the Creative Commons Attribution License (CC BY). The use, distribution or reproduction in other forums is permitted, provided the original author(s) and the copyright owner(s) are credited and that the original publication in this journal is cited, in accordance with accepted academic practice. No use, distribution or reproduction is permitted which does not comply with these terms.